Suppressing the Spreading of Continuum Wave Packets via Chirped Laser Pulses†

Corneliu Manescu,‡ Jeffrey L. Krause,‡ Klaus B. Møller,§ and Niels E. Henriksen*,§

Quantum Theory Project, University of Florida, P.O. Box 118435, Gainesville, Florida 32611-8435, and Department of Chemistry, Building 207, Technical University of Denmark, DK-2800 Kgs. Lyngby, Denmark

Received: March 1, 2004; In Final Form: April 16, 2004

We investigate the focusing, that is, the reversing of spreading of continuum wave packets created with chirped laser pulses in the weak-field limit. Focusing can be accomplished when a negative position−momentum correlation is created in the wave packet. Specializing to constant and linear (repulsive) potentials, we show analytically that in a constant potential wave packet spreading can be compensated with positively chirped laser pulses, whereas in the linear potential negatively chirped laser pulses are required, in the short-pulse limit. The analytical results for the linear potential are supported by numerical simulations. The results are discussed in the context of a classical model for wave packet focusing.

1. Introduction

When an atom or molecule interacts with an appropriate ultrafast laser pulse, a wave packet, or time-dependent superposition state, is created. Wave packets are quantum mechanical objects that exhibit a host of exotic features. For example, given a chosen initial state, one can imagine designing laser pulses with the aim of creating wave packets that steer a system into a specific target state, including states in which matter is transformed into a desired product.[1−3] On the experimental side, laser fields with complex pulse shapes can now be created routinely.[4−7] Furthermore, using the concept of laboratory feedback control,[8] it is possible to obtain control without any prior knowledge of the system Hamiltonian. This procedure is based on the feedback from an observed experimental signal and an algorithm that iteratively improves the applied femtosecond laser pulse. Several applications of this approach have been published recently.[9−14]

The present work, in line with refs 15−19, is an exploratory study with the aim of analyzing and understanding the type of dynamics that can be induced by ultrashort laser pulses. In particular, we consider the simplest type of phase modulation that leads to (nontrivial) pulse shaping, which is a quadratic frequency sweep of the phase. In the time domain, this is equivalent to a linear chirp of the pulse. Chirped pulses have now been applied in several experiments.[20−22] For example, pulses with negative chirps, in which frequency decreases as a function of time, have been shown to enhance vibrational ladder climbing compared to unchirped pulses.[22]

Wave packet dynamics in atoms and small molecules has an appealing, if deceptive, simplicity. Previous theoretical work has shown that when a continuum wave packet is created with a transform-limited, Gaussian pulse, the wave packet spreads; that is, the uncertainty in position increases with time. However, when the continuum wave packet is created with a positively chirped pulse,[23−25] the wave packet focuses, thus counteracting the "natural tendency" to spread. Alternatively, if the wave packet is excited in a molecule with a negatively chirped pulse in the bound region of an excited-state potential, the wave packet focuses after one recoil from the turning point of the potential. Some of these predictions of wave packet focusing have now been observed experimentally.[24]

The early work on wave packet focusing[23,24] led to the development of a simple, classical model for the focusing mechanism, that has formed the basis for interpreting many subsequent experimental and theoretical results. This classical model was based on the idea that high-energy components of a wave packet travel faster than low-energy components. Hence, to create a focused wave packet with an out-going momentum (that is, momentum directed away from the Franck−Condon region), a positive chirp should be applied. This causes the low-energy portions of the wave packet to be created before the high-energy components. When the high-energy components "catch up" with the low-energy components, the wave packet focuses. This mechanism is operative in both the continuum (termed previously the "cannon"), and the bound region of a potential (the "paddle-ball"). With a negatively chirped pulse, a focused wave packet with momentum directed toward the Franck−Condon region (the "reflectron") is formed in the bound region of a potential. In this case, the high-energy components of the wave packet should be created first, because they must travel a longer distance to the target region than the lower energy components. Note that this picture assumes that the high- and low-energy components start at the same position.

The classical model describes much of the salient physics. However, no classical argument can capture completely the detailed quantum mechanical effects of constructive and destructive interference that form the basis for wave packet dynamics. The purpose of the present work is to analyze the mechanism of wave packet focusing in greater detail, both analytically and numerically. As shown below, the results confirm, in some cases, the simple classical model and contradict it in others.

In the next section, we review the theoretical framework needed in order to describe the wave packet created by a laser pulse. In Section 3, we consider wave packet focusing in linear (including constant) potentials. For such potentials, analytical expressions provide intimate insights on the dynamics. In Section 4, we elaborate on simple arguments based on classical

† Part of the "Gert D. Billing Memorial Issue".
‡ University of Florida.
§ Technical University of Denmark.

10.1021/jp049077q CCC: $27.50
Published on Web 05/28/2004

dynamics with the aim of providing a rationalization of the results. Section 5 presents numerical studies of focusing in linear repulsive potentials. Finally, conclusions and perspectives are presented in Section 6.

2. The Promoted State Generated via a Laser Pulse

We consider an electronic transition in a molecule, from electronic state "1" to state "2". Within the electric-dipole approximation and first-order perturbation theory for the interaction with an electromagnetic field, the state vector associated with the nuclear motion in electronic state "2" is given by (at times, t, when the laser pulse has vanished)[26-28]

$$|\chi_2(t)\rangle = \exp(-i\hat{H}_2 t/\hbar)\,|\chi_2\rangle \tag{1}$$

Here, $|\chi_2\rangle$ is the *promoted state*

$$|\chi_2\rangle = \frac{i}{\hbar}\int_{-\infty}^{\infty} dt' e^{-i\epsilon_0 t'/\hbar} E(t')\exp(i\hat{H}_2 t'/\hbar)\,|\phi\rangle \tag{2}$$

where $E(t)$ is the laser field and

$$|\phi\rangle = \mu_{12}\,|\chi_1\rangle \tag{3}$$

is the Franck−Condon wave packet. In this expression, $|\chi_1\rangle$ is the initial stationary nuclear state in electronic state "1" with energy ϵ_0 and μ_{12} is the projection of the electronic transition dipole moment on the polarization vector of the electric field.

The target, $|\chi_{foc}(t_{foc})\rangle$, is a focused state a time $t = t_{foc}$. To generate this state, we invert eq 1 to obtain $|\chi_2\rangle$

$$|\chi_2\rangle = \exp(i\hat{H}_2 t_{foc}/\hbar)\,|\chi_{foc}(t_{foc})\rangle \tag{4}$$

by propagating the focused target state backward in time to obtain the corresponding promoted state in the Franck−Condon region. The goal, then, is to find the laser pulse that best creates this promoted state.

3. Spreading and Focusing of Wave Packets

We consider a one-dimensional system described by the Hamiltonian $\hat{H} = \hat{p}^2/(2m) + V(x)$. The time evolution associated with the variance (uncertainty) in position, is given by

$$\frac{d}{dt}[(\Delta x)_t^2] = \frac{2}{m}[\langle x\hat{p} + \hat{p}x\rangle/2 - \langle x\rangle\langle\hat{p}\rangle] \equiv (2/m)r_t \tag{5}$$

where r_t is the covariance (or correlation coefficient) of the position and momentum. Thus, when $r_t > 0$ the wave packet will spread, whereas $r_t < 0$ implies that the wave packet will focus (i.e., contract). At times when the correlation r_t is zero, the width is either in a local minimum or a local maximum.

Specializing to a linear potential

$$V(x) = V(x_0) - \alpha(x - x_0) \tag{6}$$

eq 5 can be integrated to give

$$(\Delta x)_t^2 = (\Delta x)_0^2 + [(2/m)r_0]t + [(\Delta p)_0^2/m^2]t^2 \tag{7}$$

Thus, for $r_0 \geq 0$, the wave packet spreads continuously, whereas for $r_0 < 0$, $(\Delta x)_t^2$ has a minimum as a function of time; that is, when a negative correlation exists between the position and momentum in the wave packet at $t = 0$ the wave packet will (initially) focus. Differentiating eq 7 gives

$$r_t = r_0 + [(\Delta p)_0^2/m]t \tag{8}$$

Hence, for a linear potential, dr_t/dt is always positive, signifying that for large enough times a wave packet always spreads. The only way to achieve focusing is to have a wave packet that initially has a negative position−momentum correlation, $r_0 < 0$. In this situation the wave packet will contract until the time t_{foc}, when the correlation r_t is zero, that is

$$t_{foc} = m|r_0|/(\Delta p)_0^2 \tag{9}$$

after which it starts spreading. The minimum width (at time t_{foc}) is given by

$$(\Delta x)_{t_{foc}}^2 = (\Delta x)_0^2 - r_0^2/(\Delta p)_0^2 \tag{10}$$

3.1. Gaussian Wave Packets in Linear Potentials. For a linear potential, we can construct the promoted state in eq 4 analytically. If the focused target state is chosen as a (minimum uncertainty) Gaussian, the promoted state is also a Gaussian. By analyzing the properties of the promoted state, we can gain insight on how this promoted state might be created via an ultrashort pulse.

Note that a linear potential is a reasonable approximation in the Franck−Condon region of diatomic molecules or for wave packets moving at high kinetic energies such that the potential has a negligible effect.

3.1.1. The Promoted State. Consider a Gaussian wave packet[29,30]

$$\psi_G(x, t) = \exp\left\{\frac{i}{\hbar}[A_t(x - x_t)^2 + p_t(x - x_t) + s_t]\right\} \tag{11}$$

where x_t and p_t are the expectation values of position and momentum, respectively, and A_t is a complex parameter related to the width and the correlation between position and momentum

$$A_t = \frac{2r_t + i\hbar}{4(\Delta x)_t^2} \tag{12}$$

where $r_t = (\hbar/2)\mathrm{Re}(A_t)/\mathrm{Im}(A_t)$.

The uncertainty in the momentum is given by

$$(\Delta p)_t^2 = 4|A_t|^2(\Delta x)_t^2 = \frac{\hbar^2/4 + r_t^2}{(\Delta x)_t^2} \tag{13}$$

and therefore a focused Gaussian wave packet ($r_t = 0$) is a minimum uncertainty state.

The Wigner phase-space function associated with the Gaussian is

$$\Gamma_G(x, p, t) = \frac{1}{\pi\hbar}\exp[-2(\Delta p)_t^2(x - x_t)^2/\hbar^2 - 2(\Delta x)_t^2(p - p_t)^2/\hbar^2 + 4r_t(x - x_t)(p - p_t)/\hbar^2] \tag{14}$$

A contour plot of this function is shown in Figure 1.

Now, for the case of a linear (including a constant) potential, eq 6, the time evolution of A_t is given by[29]

$$A_t = \frac{A_0}{1 + (2A_0/m)t} \tag{15}$$

where A_0 is A_t at $t = 0$. From this relation, eqs 7 and 8 can be derived easily.

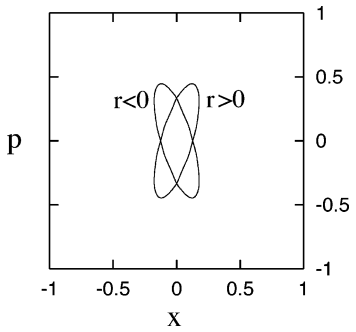

Figure 1. Phase-space plot of the Wigner function for a Gaussian wave packet. Two contours are shown. The contour "$r < 0$" corresponds to a Gaussian with a negative position−momentum correlation, whereas the contour "$r > 0$" corresponds to a Gaussian with a positive position−momentum correlation.

Inserting eq 13 into eqs 9 and 10 we obtain, for a Gaussian with $r_0 < 0$

$$t_{\text{foc}} = m(\Delta x)_0^2 \frac{|r_0|}{\hbar^2/4 + r_0^2} \tag{16}$$

and

$$(\Delta x)_{t_{\text{foc}}}^2 = (\Delta x)_0^2 \frac{\hbar^2/4}{\hbar^2/4 + r_0^2} \tag{17}$$

We now derive the reverse relations: Given the focusing time t_{foc} and the associated width $(\Delta x)_{t_{\text{foc}}}^2$, what are r_0 and $(\Delta x)_0^2$ of the promoted state? Inverting the above relations, we find

$$r_0 = -\frac{\hbar^2}{4m} \frac{t_{\text{foc}}}{(\Delta x)_{t_{\text{foc}}}^2} \tag{18}$$

and

$$(\Delta x)_0^2 = (\Delta x)_{t_{\text{foc}}}^2 + \frac{\hbar^2}{4m^2} \frac{t_{\text{foc}}^2}{(\Delta x)_{t_{\text{foc}}}^2} \tag{19}$$

We see that for a chosen width of the focused wave packet, $(\Delta x)_{t_{\text{foc}}}$, a large value of t_{foc} implies that the width as well as the absolute value of the position−momentum correlation of the promoted state must be large.

Note that t_{foc} is related to the expectation value of the position for the focused state x_{foc}

$$x_{\text{foc}} = x_0 + \alpha t_{\text{foc}}^2/(2m) \tag{20}$$

where α is the slope of the potential and $p_0 = 0$.

Above we considered the A_0 associated with the promoted state obtained by backward propagation of the target state. Thus, we can create a desired focused target state at *any* selected time or position x_{foc}, provided we can generate the associated promoted state. A somewhat less ambitious goal is to consider a promoted state with a fixed width, $(\Delta x)_0$, and to find the form of this state that produces a maximum focusing time, t_{foc}. Maximizing t_{foc} in eq 16 with respect to r_0 for a fixed value of $(\Delta x)_0$ gives the maximum focusing time

$$t_{\text{foc}}^{\max} = \frac{m}{\hbar}(\Delta x)_0^2 \tag{21}$$

that can be achieved for an initial position−momentum correlation of the promoted state $r_0 = -\hbar/2$. We see again that to obtain a large value of t_{foc} a delocalized promoted state is required (obtained, for example, by excitation from an excited state). To calculate the width of the focused packet at the target time, we use eq 17 to find

$$(\Delta x)_{t_{\text{foc}}^{\max}}^2 = (\Delta x)_0^2/2 \tag{22}$$

This equation shows that when the focusing time is maximal, focusing is limited to half of the initial width of the promoted state. As an example, assume that $(\Delta x)_0^2 = \hbar/(2m\omega)$ as in a harmonic vibrational ground state. Then $t_{\text{foc}}^{\max} = 1/(2\omega)$, which corresponds to $P/(4\pi)$ where P is the vibrational period; that is, $t_{\text{foc}}^{\max}$ is just a small fraction of the vibrational period.

From the analysis above, we see that obtaining a large value of the focusing time requires a delocalized promoted state. From eq 2, it is clear that a delocalized promoted state *cannot* be created with a short pulse.

3.1.2. Promoted State via an Ultrashort Laser Pulse. In this section we investigate the properties of the promoted state created by a chirped, ultrafast laser pulse. The electric field is written in the form

$$E(t) = E_0 \exp[-t^2/(2\tau^2) - \mathrm{i}\omega_0 t - \mathrm{i}\beta t^2/2] \tag{23}$$

The instantaneous frequency is $\omega(t) = \omega_0 + \beta t$, where ω_0 is the carrier frequency, and β is the linear chirp of the pulse. The Fourier transform of the electric field is given by

$$\tilde{E}(\omega) = E_0' \exp[-\tau_0^2(\omega - \omega_0)^2/2 + \mathrm{i}\beta_0(\omega - \omega_0)^2/2] \tag{24}$$

where $\tau_0^2 = \tau^2/(1 + \tau^4\beta^2)$ and $\beta_0 = \beta\tau^4/(1 + \tau^4\beta^2)$.

The initial state is assumed to be a Gaussian and the variation of the electronic transition dipole moment over the width of this Gaussian is neglected, that is, $\phi(x) = N \exp[-(x - x_0)^2/4(\Delta x)_g^2]$. When the initial state and the electric field (in the limit $\tau \to 0$) are inserted into eq 2 the time-evolution operator is split into two parts. One part depends on the kinetic energy operator, and one depends on the potential. The action of the kinetic energy operator can be neglected (since the spreading of the initial state during the interaction with the pulse is negligible), and so only the part which depends on the potential is retained.

For $\hbar\omega_0 = V(x_0) - \epsilon_0$ (i.e., on-resonant excitation), we obtain a promoted state given by[31]

$$\chi_2(x) = \frac{\mathrm{i}}{\hbar}\tilde{E}\left[\frac{V(x) - \epsilon_0}{\hbar}\right]\phi(x)$$
$$= \exp\left\{\frac{\mathrm{i}}{\hbar}[A_0(x - x_0)^2 + s_0]\right\} \tag{25}$$

where

$$\mathrm{Re}(A_0) = \frac{r_0}{2(\Delta x)_0^2} = \frac{\alpha^2}{2\hbar}\frac{\beta}{(1/\tau^2)^2 + (\beta)^2}$$

$$\mathrm{Im}(A_0) = \frac{\hbar}{4(\Delta x)_0^2} = \frac{\hbar}{4(\Delta x)_g^2} + \frac{\alpha^2}{2\hbar}\frac{1/\tau^2}{(1/\tau^2)^2 + (\beta)^2} \tag{26}$$

The above equations demonstrate that a *negative* chirp ($\beta < 0$) creates a Gaussian wave packet with a negative correlation, $r_0 < 0$ (see Figure 2). Furthermore, the promoted state is squeezed compared to the initial vibrational ground state ($(\Delta x)_g > (\Delta x)_0$), resulting in a small t_{foc}. Note that for $\alpha = 0$ (i.e., a

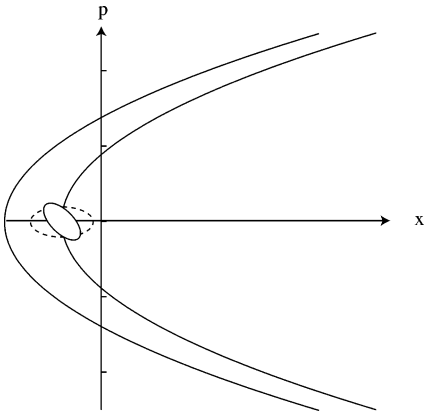

Figure 2. Phase-space plot of the Wigner function in a linear potential, created with an ultrashort negatively chirped pulse. The dashed (closed) curve is a contour of the Wigner function of the initial Gaussian, the solid (closed) curve is the Wigner function of the Gaussian created with an ultrashort pulse with negative chirp. The parabolas are constant energy contours corresponding to two different total energies. The center of the Gaussian wave packet follows such a trajectory.

constant potential) the promoted state generated by an ultrashort pulse is identical to the initial state, and focusing is not possible in the ultrashort-pulse limit.

The time t_{foc} at which the wave packet will focus can be determined using eq 16 to give

$$t_{foc} = \frac{2m(\alpha')^2(\Delta x)_g^2}{\hbar}\frac{|\beta/2|}{a^2 + (\beta/2)^2} \tag{27}$$

where $\alpha' = \alpha(\Delta x)_g/\hbar$, and $a = (\alpha')^2 + 1/(2\tau^2)$. The focusing time depends on the chirp, and the maximum value of t_{foc} is obtained when $\beta = \beta_{max} = -2a$. For this value of the chirp

$$t_{foc}^{max} = \frac{m(\Delta x)_g^2/\hbar}{1+b} \tag{28}$$

where $b = \hbar^2/(2(\Delta x)_g^2\alpha^2\tau^2)$. The associated uncertainty in position is given by

$$(\Delta x)^2_{t_{foc}^{max}} = \frac{1+2b}{1+b}(\Delta x)_g^2/2 \tag{29}$$

In general, if the chirp has a value $\beta = k\beta_{max}$, using eqs 26−28 we obtain a focusing time

$$t_{foc} = \frac{2k}{1+k^2}t_{foc}^{max} \tag{30}$$

and associated uncertainty of

$$(\Delta x)^2_{t_{foc}} = \frac{k(1+2b)}{k^2(1+b)+b}(\Delta x)^2_{t_{foc}^{max}} \tag{31}$$

where, as expected, $t_{foc} < t_{foc}^{max}$. Given a ground-state wave packet, and an excited linear potential, the formulas in eqs 30 and 31 allow us to predict the focusing time and the associated uncertainty for any pulse with parameters τ and β.

The expressions in eqs 28 and 29 are quite similar to the results in eqs 21 and 22. They are not identical, however, since they represent the connection between the focusing quantities, t_{foc} and $(\Delta x)_{t_{foc}^{max}}$, and the ground-state (instead of promoted state) width, $(\Delta x)_g$, the pulse width, τ, and the potential slope, α. Furthermore, the real and imaginary parts of A_0 in eq 26 are not independent since they both depend on the chirp parameter. Note that in eqs 28 and 29 the chirp is not a parameter, since it is implicitly set by the condition for a maximum t_{foc} ($\beta = -2a$).

Rather than maximizing the focusing time, we can choose to maximize the effect of the focusing. To do this, we define a focusing parameter, f, as the ratio between the variance of the promoted state, $(\Delta x)_0^2$, and the variance at the focusing time, $(\Delta x)^2_{t_{foc}}$. With the use of eq 17, f is given by

$$f = \frac{(\Delta x)_0^2}{(\Delta x)^2_{t_{foc}}} = 1 + (2r_0/\hbar)^2 \tag{32}$$

As can be seen in this equation, to maximize f, we must maximize r_0 (i.e., the initial correlation between position and momentum) with respect to the chirp. By taking the ratio $\mathrm{Re}(A_0)/\mathrm{Im}(A_0)$, and setting $\beta = k\beta_{max}$, where k is a positive constant, and β_{max} is defined below eq 27, we obtain

$$\left|\frac{2r_0}{\hbar}\right| = \frac{k}{k^2(1+b)+b} \tag{33}$$

where b is defined above. The maximum of this ratio is obtained for $k = \sqrt{b/(1+b)}$, which implies that

$$f_{max} = 1 + [4(b+b^2)]^{-1} \tag{34}$$

Note that, in the above formulas, both t_{foc}^{max} and f_{max} depend on the parameter b, which implies that all cases with the same value of $\alpha^2\tau^2$ are equivalent.

3.2. Promoted State in a Constant Potential. The formulas in the preceding section were derived in the short-pulse limit. For pulses with a finite (nonzero) width, the explicit expression for the promoted state is extremely complicated and not reported here. However, one important observation can be made. The promoted state is in general not a Gaussian, which in turn implies that the linearly chirped electric field in eq 23 cannot guide the system into a Gaussian (minimum uncertainty) target state.

To simplify the analysis, we consider a constant potential, using the form of the laser field in eq 23. Setting the excited-state potential $V(x) = V$, we begin in the momentum-space representation and obtain from eq 2

$$\tilde{\chi}_2(p) = \frac{i}{\hbar}\tilde{E}\left(\frac{p^2/2m + V - \epsilon_0}{\hbar}\right)\tilde{\phi}(p) \tag{35}$$

Assuming again that the initial state is a Gaussian, $\tilde{\phi}(p) = N\exp[-p^2/4(\Delta p)_g^2]$, it can be shown that

$$r_0 = -\frac{\hbar\beta\tau^2}{2}\left[1 - \frac{(\Delta p)_0^2}{(\Delta p)_g^2}\right] \tag{36}$$

This relation shows, in contrast to the above analysis, that the ratio r_0/β can be either positive or negative, which implies that either a negative or positive chirp might be required to create a focused wave packet; depending on the width in momentum

space of the promoted state relative to the initial state. For $\omega_0 > V - \epsilon_0$, we find

$$\left|\tilde{E}\left(\frac{p^2/2m + V - \epsilon_0}{\hbar}\right)\right|^2 = |E_0'|^2 \exp\left[-\tau_0^2\left(\frac{p^2/2m + V - \epsilon_0 - \hbar\omega_0}{\hbar}\right)^2\right] \quad (37)$$

In the ultrashort-pulse limit, $\tau_0 \to 0$, the Fourier transform of the electric field approaches a constant, and from eq 36 we observe, as previously, that the position−momentum correlation vanishes. For a long pulse, eq 37 is double-peaked, around the values $\pm p(\omega_0) \equiv \pm\sqrt{2m(V-\epsilon_0-\hbar\omega_0)}$, and therefore the width of this function is, roughly speaking, given by $p(\omega_0)$ Hence, to obtain a focused wave packet ($r_0 < 0$) eq 36 suggests that

$$\beta < 0, \quad \text{for } p(\omega_0) > (\Delta p)_g$$
$$\beta > 0, \quad \text{for } p(\omega_0) < (\Delta p)_g \quad (38)$$

In a recent paper,[32] a free particle model was used to describe the creation of electronic wave packets, and it was argued that the spreading of such a wave packet can be compensated only by a positively chirped pulse. However, in ref 32 only electrons with positive momentum were considered. In this case, $(\Delta p)_0$ is always smaller than $(\Delta p)_g$, and according to eq 36 focusing can only be obtained with a positive β.

In the next section, we discuss a simple classical model of the dynamics, with the aim of providing an intuitive rationalization of the analytical results, especially the dependence on the sign of the chirp.

4. Qualitative Arguments Based on Classical Dynamics

In the quantum picture, the dynamics is given by the excited-state wave function, which according to eqs 1 and 2 can be written in the form

$$\chi_2(x, t) = \frac{i}{\hbar}\int_{-\infty}^{\infty} dt' e^{-i\epsilon_0 t'/\hbar} E(t')\phi(x, t - t') \quad (39)$$

where $\phi(x, t - t') = \langle x \mid \exp[-i\hat{H}_2(t - t')/\hbar] \mid \phi\rangle$. Thus, the excited-state wave function can be thought of as a coherent superposition of Franck−Condon wave packets created in the upper state at times t' with different weighting factors (given by $E(t')$) and phases. At time t, each of these wave packets in the superposition has evolved for a time $t - t'$. The promoted state wave function is obtained by setting $t = 0$ in eq 39. Since the initial state is a stationary state in the electronic ground state "1", the expectation value of the momentum associated with $\phi(x, 0)$ is zero. Furthermore, when the description in Section 3.1.2 is extended to "off-resonant" excitation $\hbar\omega_0 > V(x_0)$ or $\hbar\omega_0 < V(x_0)$, the maximum in the amplitude of the wave packet is displaced to $x < x_0$ and $x > x_0$, respectively.[31] With a pulse of nonzero duration (and its associated frequency distribution), a chirped pulse can be viewed as a series of short pulses with time-dependent center frequencies.

For the purpose of interpreting the quantum results, classical arguments are often applied.[23,24] To do this, we neglect the initial momentum and position distribution of the Franck−Condon wave packets and consider the dynamics of classical trajectories on the excited-state surface. All trajectories begin with zero momentum, and the objective is for the trajectories to evolve to the position x_{foc} at time t_{foc}. The focusing time t_{foc} and its dependence on the initial position is, for a linear potential, given by eq 20. On this potential all trajectories experience the same acceleration. As a result, the trajectories excited with high frequencies must be excited first—they must travel a longer distance in order to reach x_{foc}; that is, a pulse with a *negative* chirp is required. Note the differences in this argument compared to the one presented in the Introduction, where all trajectories were assumed to start out at the same position. Figure 3a shows the promoted state constructed as described above. This plot is an approximate picture of the Wigner function, and since the dynamics in phase space for a linear potential can be described exactly in terms of classical trajectories, we see that the time evolution of the promoted state leads to focusing in coordinate space. This picture should be valid also in a real nonlinear potential as long as we consider focusing within the Franck−Condon region.

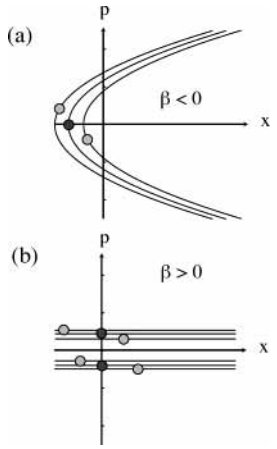

Figure 3. Phase-space plot of the "Wigner function" in a linear potential (a) and constant potential (b), respectively. The density in phase space is the promoted state created with a negatively (a) or positively (b) chirped pulse. These pictures are obtained within a "classical approximation", as detailed in the text. A pulse with a Gaussian envelope function centered around $t = 0$ has been used, and the contributions to the phase-space density of the promoted state have been sketched at three times (chosen symmetrically around $t = 0$). The shading of the "balls" reflects the amplitude of the Gaussian envelope. The parabolas (a) and straight lines (b) are constant energy contours (at equidistant energies) corresponding to different total energies.

In the special case of a constant potential the classical picture is slightly different. Here all the trajectories begin at the same position but with different nonzero momenta determined by the instantaneous center frequency of the field. Figure 3b shows the promoted state generated by a positively chirped pulse, that creates the parts with (numerically) small momenta first. If, for example, we consider the part with positive momentum, we see that time evolution leads to focusing since the high-momentum part will catch up with the low-momentum part. Note that these predictions coincide with the exact results described in the previous section, with one exception—the "turnover" to a negative chirp for a constant potential cannot be described within the classical picture.

Next, consider a nonlinear, for example, exponential potential and focusing in the asymptotic region far from the Franck−Condon region. In this case, trajectories excited with high frequencies will experience a higher final speed than the trajectories excited with lower frequencies. Thus, although trajectories excited with high frequencies must travel a longer distance to reach x_{foc}, they will do so with a higher speed. Consequently, it might be necessary to first excite the trajectories with the smallest final speed (total energy); that is, a *positive* chirp should be required. Depending on the value of x_{foc}, a

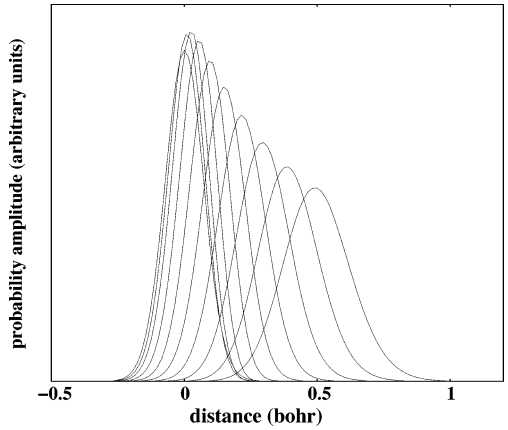

Figure 4. Snapshots of the wave packet evolution for the maximum focusing time case. The width of the initial state, $(\Delta x)_g = 0.08$ bohr, corresponds to the width of the ground vibrational state of ICN. The pulse width, $\tau = 3.0$ fs, and the value of the chirp, $\beta = -0.248$ fs^{-2}, are chosen to maximize the focusing time. The focusing time, t_{foc}, is 3.4 fs, according to the analytical formulas. The focusing, *f*, for this case is 1.08. From left to right the propagation times are 0, 1.9, 3.4, 5.3, 7.3, 9.2, 11.1, 13.1, 15.0, and 16.9 fs.

crossover from negative to positive chirp might be anticipated, connecting the analysis in this work with previous work.[23,24]

Finally, it should be remembered that the classical model neglects the initial position and momentum distributions of the Franck−Condon wave packet. Furthermore, dynamics in phase space can be described exactly in terms of classical trajectories only for potentials that are linear or harmonic. As a result, the simple explanations discussed in this section are not expected to be highly reliable for a general potential.

5. Numerical Results

In this section, we present the results of several numerical simulations designed to test the range of validity of the analytical expressions derived in Section 3.1.2. The numerical results are obtained via a direct integration of the time-dependent Schrödinger equation. As a model system, we consider the photodissociation of the molecule ICN. In this molecule, dissociation occurs along the I−C coordinate, and the CN bond can be considered rigid. A linearization of one of the purely repulsive excited electronic states of ICN[33] in the Franck−Condon region leads to $\alpha = 0.08$ bohr^{-1}, where α is defined in eq 6. The linear approximation is reasonable for the first 20−25 fs.[33] At longer times, the linear potential is simply a model potential. For the ground vibrational state of ICN, $(\Delta x)_g = 0.08$ bohr. The reduced mass, *m*, of ICN is 21.6 amu.

Figure 4 shows snapshots of the wave packet dynamics for the maximum focusing time case for the ground vibrational state of ICN. The pulse width, τ, is 3.0 fs, and the chirp, β, is the optimal value of -0.248 fs^{-2}. With these parameters, eq 28 predicts that $t_{foc}^{max} = 3.4$ fs, and the location at which the focusing occurs is $x_{foc} = 0.02$ bohr. As can be seen in the figure, these predictions agree perfectly with the numerical results. The focusing, *f*, for this case is modest, with $f = 1.08$.

While the results in Figure 4 confirm the validity of the analytical formulas, they are somewhat disappointing in the sense that the maximum focusing time occurs just after the end of the pulse, and the focusing distance is very close to the Franck−Condon point. The reason for this difficulty can be seen by examining eqs 28 and 29. The maximum focusing time, for a fixed slope of the potential and mass, depends on $(\Delta x)_g$ and τ. The maximum possible t_{foc}^{max} is obtained as $\tau \rightarrow \infty$, in which case $t_{foc}^{max} \propto (\Delta x)_g^2$. Consequently, when $(\Delta x)_g^2$ is small, t_{foc}^{max} is small, and x_{foc} must also be small. With a short pulse, both effects are compounded.

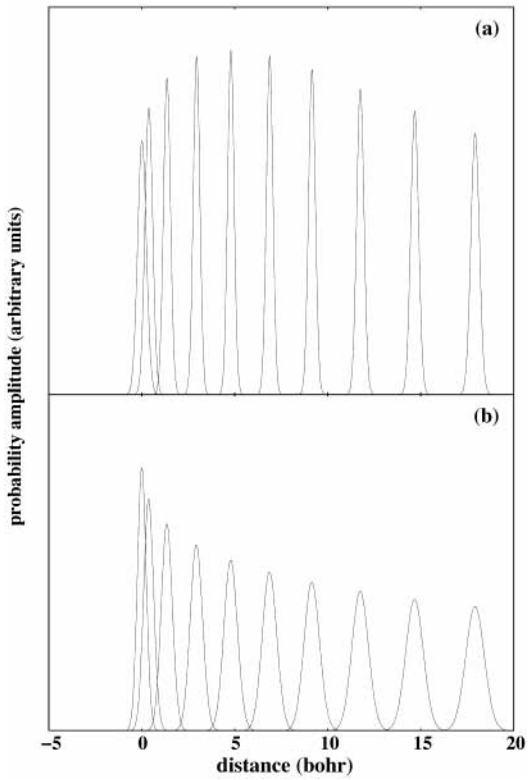

Figure 5. (Panel a): Snapshots of the wave packet evolution for the maximum focusing time case. The width of the initial state, $(\Delta x)_g = 0.24$ bohr, corresponds to the width of the $\nu = 4$ excited vibrational state of ICN. The pulse width, $\tau = 4.2$ fs, and the value of the chirp, $\beta = -1.318$ fs^{-2}, are chosen to maximize the focusing time. The focusing time, t_{foc}, is 52.5 fs, according to the analytical formulas. The focusing, *f*, for this case is 1.37. From left to right the propagation times are 0, 14.5, 27.8, 41.1, 52.5, 62.9, 72.6, 82.2, 91.9, and 101.6 fs. (Panel b): Same as panel a, except that the sign of the chirp is reversed; that is, $\beta = 1.318$ fs^{-2}.

To obtain more impressive focusing results, we consider $(\Delta x)_g = 0.24$ bohr, which corresponds to the variance associated with an excited vibrational state of ICN with $\nu = 4$.[30] Figure 5a shows snapshots of the wave packet propagation for t_{foc}^{max}, with pulse parameters as listed in the caption. In this case, the focusing time is 52.5 fs, which is well after the end of the excitation pulse, and the focusing position is 4.78 bohr, which is well beyond the Franck−Condon region. The focusing, *f*, is 1.37. Once again, the agreement with the analytical formulas is perfect. While the focusing in Figure 5a appears to be relatively moderate, if the sign of the chirp is reversed, as in Figure 5b, the wave packet dynamics is completely different. The wave packet spreads continuously, and the width at the target time is much greater than in the negatively chirped case. The comparison of parts a and b of Figure 5 shows that the negative chirp does indeed counteract the natural tendency for wave packets to spread.

Figure 6 shows snapshots of the dynamics for the same situation as in Figure 5, except that the chirp has be chosen according to eq 34 such that the focusing is maximized. The focusing, *f*, is 2.56 and the wave packet is focused at $t_{foc} = 21.0$ fs, in the region in which the linear approximation to the excited-state potential of ICN is reasonable.

Figure 7 shows snapshots of the dynamics for the maximum focusing case, where the pulse width, τ, is chosen to be 24.2

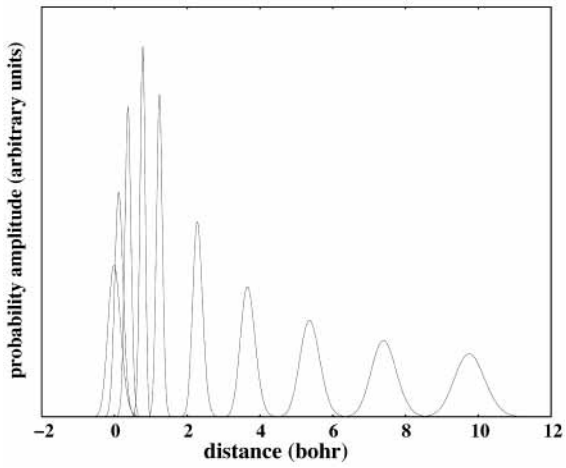

Figure 6. Same as in Figure 5, except that the chirp has been chosen to maximize the focusing, $\beta = -0.275$ fs^{-2}. The focusing time, t_{foc}, is 21.0 fs, according to the analytical formulas. The focusing, *f*, for this case is 2.56. From left to right the propagation times are 0, 8.5, 14.5, 21.0, 26.6, 36.3, 46.0, 55.6, 65.3, and 75.0 fs.

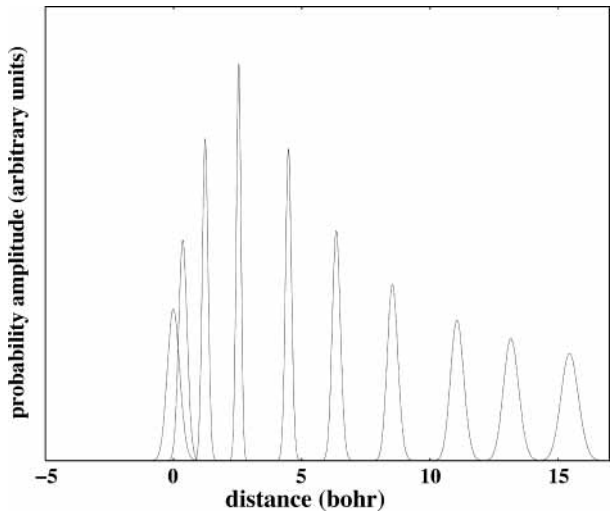

Figure 7. Snapshots of the wave packet evolution for the maximum focusing case. The width of the initial state, $(\Delta x)_g = 0.24$ bohr, corresponds to the width of the $v = 4$ excited vibrational state of ICN. The pulse width, $\tau = 24.2$ fs, and the value of the chirp, $\beta = -0.513$ fs^{-2}, are chosen to maximize the focusing. The focusing time, t_{foc}, is 38.2 fs, according to the analytical formulas. The focusing, *f*, for this case is 2.70. From left to right the propagation times are 0, 14.5, 26.6, 38.2, 50.8, 60.5, 70.1, 79.8, 87.1, and 94.3 fs.

fs, a much longer pulse than in Figure 5. The focusing time is 38.2 fs, which, as expected, is considerably shorter than the maximum focusing time. However, the focusing, *f*, is 2.70, which is greater than in the previous case. Once again, the agreement between the analytical predictions and the numerical results is excellent.

The formulas derived in Section 3.1.2 were obtained in the limit $\tau \rightarrow 0$. It is natural, then, to question at what point does this approximation becomes invalid. In the short-pulse limit, the promoted state is Gaussian (for a Gaussian initial state). We find that for a given β, as τ increases the promoted state becomes increasingly non-Gaussian. This is an indication of the breakdown of the short-pulse approximation. Interestingly, though, we find, even for moderately distorted promoted states, the analytical predictions for t_{foc} and x_{foc} remain valid. We suspect that this is due to the special nature of the linear potential. Future work will investigate this effect in greater detail and will consider more complicated, nonlinear forms of the potential.

6. Conclusions

We investigated the focusing of continuum wave packets created with chirped laser pulses in the weak-field limit. We demonstrated that focusing can be accomplished when a negative position−momentum correlation is created in the wave packet. Specializing to constant and linear (repulsive) potentials, we showed that if the focused target state is chosen as a minimum uncertainty Gaussian the promoted state, created by the laser pulse, must also be a Gaussian. Furthermore, with a target state located far from the Franck−Condon region, a delocalized promoted state is required, which in turn requires a pulse with a long duration.

With a Gaussian pulse shape with linear chirp, the promoted state is non-Gaussian, except in the limit of an ultrashort Gaussian pulse. We showed analytically that in a constant potential wave packet spreading can be compensated with positively chirped laser pulses, whereas in the linear potential negatively chirped laser pulses are required, in the short-pulse limit. Numerical simulations showed that the formulas derived in the short-pulse limit worked surprisingly well also for pulses of longer duration (fwhm ∼40−50 fs). We elaborated on a classical model for wave packet focusing and showed that most of the predictions could be rationalized within this model.

As mentioned in the Introduction, it was found in earlier numerical simulations on wave packet focusing[23,24] that focusing of a continuum wave packet far from the Franck−Condon region could be accomplished with a positively chirped pulse. Since we found that negatively chirped laser pulses compensated for the spreading in a linear repulsive potential, it is clear that the nonlinearity of real potentials must play a role. Thus, in order to fully account for the focusing of wave packets we must study focusing in nonlinear potentials, for example, using the exponential (model) ICN.[33] Future work will address the crossover from negative to positive chirp in nonlinear repulsive potentials depending on the chosen position of the focused wave packet x_{foc}, the curvature of the potential, and the parameters of the laser pulse.

Acknowledgment. We are pleased to dedicate this paper to the memory of Gert Billing with whom it was always a pleasure to interact, both scientifically and personally. J.L.K. would like to thank the Danish-American Fulbright commission for their support of his sabbatical leave in Denmark, where some of this work was completed.

References and Notes

(1) Rice, S. A.; Zhao, M. *Optical Control of Molecular Dynamics*; Wiley: New York, 2000.
(2) Brumer, P.; Shapiro, M. *Annu. Rev. Phys. Chem.* **1992**, *43*, 257.
(3) Henriksen, N. E. *Chem. Soc. Rev.* **2002**, *31*, 37.
(4) Warren, W. S. *Science* **1988**, *242*, 878.
(5) Weiner, A. M.; Heritage, J. P. *Rev. Phys. Appl.* **1987**, *22*, 1619.
(6) Weiner, A. M.; Leaird, D. E.; Wiederrecht, G. P.; Nelson, K. A. *Science* **1990**, *247*, 1317.
(7) Weiner, A. M.; Leaird, D. E.; Patel, J. S.; Wullert, J. R. *Opt. Lett.* **1990**, *15*, 326.
(8) Judson, R. S.; Rabitz, H. *Phys. Rev. Lett.* **1992**, *68*, 1500.
(9) Assion, A.; Baumert, T.; Bergt, M.; Brixner, T.; Kiefer, B.; Seyfried, V.; Strehle, M.; Gerber, G. *Science* **1998**, *282*, 919.
(10) Weinacht, T. C.; Ahn, J.; Bucksbaum, P. H. *Nature* **1999**, *397*, 233.
(11) Brixner, T.; Damrauer, N. H.; Niklaus, P.; Gerber, G. *Nature* **2001**, *414*, 57.
(12) Levis, R. J.; Mekir, G. M.; Rabitz, H. *Science* **2001**, *292*, 709.

(13) Zeidler, D.; Frey, S.; Kompa, K. L.; Motzkus, M. *Phys. Rev. A* **2001**, *64*, 023420.
(14) Herek, J. L.; Wohlleben, W.; Cogdell, R. J.; Zeidler, D.; Motzkus, M. *Nature* **2002**, *417*, 533.
(15) Krause, J. L.; Schafer, K. J.; Ben-Nun, M.; Wilson, K. R. *Phys. Rev. Lett.* **1997**, *79*, 4978.
(16) Cao, J.; Bardeen, C. J.; Wilson, K. R. *Phys. Rev. Lett.* **1998**, *80*, 1406.
(17) Malinovsky, V. S.; Krause, J. L. *Chem. Phys.* **2001**, *267*, 47.
(18) Henriksen, N. E.; Møller, K. B. *J. Chem. Phys.* **2003**, *119*, 2569.
(19) Møller, K. B.; Henriksen, N. E. *Chem. Phys. Lett.* **2004**, *385*, 134.
(20) Bardeen, C. J.; Wang, Q.; Shank, C. V. *Phys. Rev. Lett.* **1995**, *75*, 3410.
(21) Jones, R. R.; Noordam, L. D. *Adv. At. Mol. Opt. Phys.* **1997**, *38*, 1.
(22) Zeidler, D.; Frey, S.; Kompa, K. L.; Motzkus, M. *J. Chem. Phys.* **2003**, *118*, 2021.
(23) Krause, J. L.; Whitnell, R. M.; Wilson, K. R.; Yan, Y.; Mukamel, S. *J. Chem. Phys.* **1993**, *99*, 6562.
(24) Kohler, B.; Yakovlev, V. V.; Che, J.; Krause, J. L.; Messina, M.; Wilson, K. R.; Schwentner, N.; Whitnell, R. M.; Yan, Y. *Phys. Rev. Lett.* **1995**, *74*, 3360.
(25) Cao, J.; Wilson, K. R. *J. Chem. Phys.* **1997**, *107*, 1441.
(26) Rama Krishna, M. V.; Coalson, R. D. *Chem. Phys.* **1988**, *120*, 327.
(27) Henriksen, N. E. *Adv. Chem. Phys.* **1995**, *91*, 433.
(28) Cao, J.; Wilson, K. R. *J. Chem. Phys.* **1997**, *106*, 5062.
(29) Heller, E. J. *J. Chem. Phys.* **1975**, *62*, 1544.
(30) Møller, K. B.; Henriksen, N. E. *J. Chem. Phys.* **1996**, *105*, 5037. *Phys. Scr.* **1997**, *55*, 542.
(31) Henriksen, N. E.; Engel, V. *Int. Rev. Phys. Chem.* **2001**, *20*, 93.
(32) Delagnes, J. C.; Bouchene, M. A. *J. Phys. B* **2002**, *35*, 1819.
(33) Williams, S. O.; Imre, D. G. *J. Phys. Chem.* **1988**, *92*, 6648.